Intracavity terahertz-wave generation in a synchronously pumped optical parametric oscillator using quasi-phase-matched GaAs

J. E. Schaar, K. L. Vodopyanov, and M. M. Fejer

Edward L. Ginzton Laboratory, Stanford University, Stanford, California 94305, USA

Received December 13, 2006; revised February 15, 2007; accepted February 19, 2007; posted February 23, 2007 (Doc. ID 78011); published April 17, 2007

We generated 1 mW of average output power at 2.8 THz (bandwidth of ~300 GHz) in a diffraction-limited beam by placing a 6-mm-long quasi-phase-matched GaAs crystal inside the cavity of a synchronously pumped optical parametric oscillator (OPO). The OPO used type-II-phase-matched periodically poled lithium niobate as a gain medium and was pumped by a mode-locked laser at 1064 nm, with a 7 ps pulse duration, 50 MHz repetition rate, and 10 W average output power. The terahertz radiation was generated by difference frequency mixing between the signal and idler waves of the near-degenerate doubly resonant OPO.

OCIS codes: 190.2620, 190.4410, 190.4970, 190.7070.

Parametric frequency downconversion of optical pulses in electro-optic (EO) crystals is a well-known method of generating terahertz (THz) radiation.[1] Potentially, it will enable compact tunable THz emitters working at room temperature, by using diode-pumped laser sources with different temporal formats: continuous-wave to femtosecond (fs) pulses. This technique can generate quasi-monochromatic THz radiation using difference-frequency generation (DFG) with two input beams[1–6] or through THz-wave parametric oscillation with a single fixed-frequency optical pump.[7–9] Alternatively, broadband THz transients can be generated by means of optical rectification (OR) of ultrashort (typically fs) laser pulses.[10–13] In Ref. 13, up to 10% optical-to-THz quantum conversion efficiency was achieved in the OR process in bulk lithium niobate with 150 fs, 500 μJ tilted-wavefront laser pulses with a 1 kHz repetition rate.

Using quasi-phase-matched (QPM) EO crystals such as periodically poled lithium niobate (PPLN) has the potential for improving optical-to-THz conversion efficiencies by increasing effective interaction lengths for both collinear[11] and surface emitting[5,12] geometries. Recently, THz-wave generation was demonstrated in QPM GaP (Ref. 6) and QPM GaAs.[14,15] In fact, III–V semiconductors are very attractive for QPM THz-wave generation because of several appealing properties, namely (i) a small THz absorption coefficient (smaller by an order of magnitude[16] than in commonly used EO crystals: $LiNbO_3$, ZnTe, and CdTe), (ii) a large coherence length due to a small mismatch between the optical-group and THz-phase velocities, and (iii) high thermal conductivity. In Ref. 6, THz waves were generated by DFG in a periodically rotated GaP stack, produced by a direct-wafer-bonding technique, which was pumped with 10 ns pulses near 1.55 μm. In Ref. 14, THz output was generated by OR using fs laser pulses and two different QPM GaAs structures: diffusion-bonded stacked GaAs (DB-GaAs) (Ref. 17) and epitaxially grown orientation-patterned GaAs (OP-GaAs).[18] By changing the GaAs QPM period (504–1277 μm) or the pump wavelength (2–4.4 μm), tunable THz output (0.9–3 THz) was generated with 3.3% quantum conversion efficiency using only 2.3 μJ pump pulses. With a Tm-based fs fiber laser ($\lambda \approx 2$ μm and 100 MHz repetition rate) as a pump source, 3 μW of average power was generated in an OP-GaAs crystal at 1.8 and 2.5 THz.[15]

In this paper, we report a 1 mW average-power THz source based on resonantly enhanced DFG in QPM GaAs. We performed efficient difference-frequency mixing, in a collinear geometry, between the signal and idler waves ($\lambda_p < \lambda_s < \lambda_i$, where p, s, and i refer to the pump, signal, and idler, respectively) inside the cavity of a synchronously pumped doubly resonant optical parametric oscillator (DRO) (Fig. 1). The pump source for the DRO was a $Nd:YVO_4$ mode-locked laser (*pico*TRAIN series, High Q Laser) with a 50 MHz repetition rate, 7 ps pulse width, 1064 nm wavelength, and 10 W average output power. The linear DRO cavity was ~3 m in

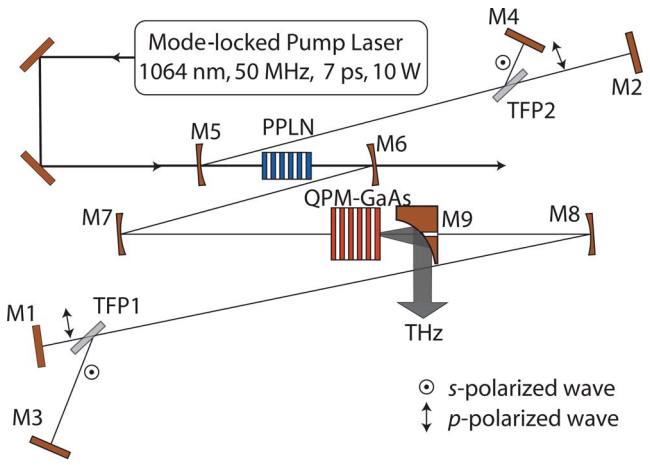

Fig. 1. (Color online) Schematic of the linear DRO with an "offset" cavity design. M1–M8, cavity mirrors; M9, off-axis parabolic mirror for THz outcoupling. Other abbreviations defined in text.

0146-9592/07/101284-3/$15.00

length with a round-trip time equal to the period between pump laser pulses. For the OPO (optical parametric oscillator) gain medium, we used an antireflection (AR) coated (for pump, signal, and idler) MgO-doped PPLN crystal, 5-mm-long, 1-mm-thick, with a QPM period of 14.1 μm. It was designed for type II ($o-oe$) QPM parametric interactions to allow narrow OPO signal and idler linewidths close to degeneracy, $\lambda_s \approx \lambda_i \approx 2\lambda_p$. The nonlinear optical coefficient for type II phase matching was 5 times less than the typical type 0 ($e-ee$) coefficient, which resulted in a parametric gain reduction factor of ~25. The spot size of the focused 1 μm pump beam in the center of the PPLN crystal was $w=30$ μm ($1/e^2$ intensity radius), while the calculated focused waists of the resonating DRO modes in the PPLN center were 57 μm. Two thin-film polarizers, TFP1 and TFP2, separated the orthogonally polarized signal and idler waves (in Fig. 1, p polarization with respect to the thin-film polarizers corresponds to an o-wave with respect to the PPLN crystal). The cavity was composed of eight mirrors, M1–M8, all of which were AR coated for the pump and high-reflection coated for the OPO signal and idler waves (2 μm band) with reflection loss <0.1%. M1 and M2 were end mirrors for the p-polarized wave, and M3 and M4 were end mirrors for the s-polarized wave. Mirrors M5 and M6 were concave with 200 mm radii of curvature, and mirrors M7 and M8 were concave with 500 mm radii of curvature. As a QPM GaAs structure we chose a 6-mm-long DB-GaAs sample with a 10 mm × 10 mm cross-section, which provided a larger aperture, compared with OP-GaAs, with typical cross-sections of 5 mm × 0.5 mm, and thus had less clipping of the THz wave. The DB-GaAs sample had a QPM period of 504 μm, and it was AR coated for the 2 μm band. It was placed near the focused signal and idler waists ($w=140$ μm, calculated) between mirrors M7 and M8. The signal and idler beams propagated along the $[1\bar{1}0]$ crystalline direction of GaAs with polarizations aligned along [001] and [110]. A gold-coated 90°-off-axis parabolic mirror, M9 (1 in. diameter and 2 in. focal length), with a 3-mm-diameter hole in its center was placed after the GaAs crystal. It fully transmitted the optical waves and allowed >90% outcoupling of the THz waves due to the large diffraction cone of the THz radiation.

To avoid backconversion of the signal and idler on the return pass in the PPLN, we made distances TFP1–M1 and TFP1–M3 unequal. To keep to the round-trip times for the signal and idler waves equal, the paths TFP2–M2 and TFP2–M4 were correspondingly adjusted (Fig. 1). In this "offset" cavity design, the signal and idler waves perfectly overlap in time during their forward pass through the PPLN; however, they do not overlap during the return pass, where otherwise the signal and the idler would backconvert to 1 μm photons by sum-frequency generation. Since the DRO resonates simultaneously at two different frequencies (signal and idler), precise control of one cavity length with respect to the other must be maintained to achieve a duty factor of 100%. By applying length dithering of 2–4 μm to one end mirror at ~100 Hz with a piezoelectric actuator, we achieve DRO oscillation with a duty factor of >30%.

The OPO tuning characteristics (Fig. 2 inset) were measured as a function of the PPLN temperature with a grating monochromator. Figure 2 shows OPO line shapes near degeneracy for two different PPLN temperatures. The FWHM linewidth was typically 1.5–3 nm for various PPLN temperatures with an average of 2 nm (130 GHz). The best THz performance in the DB-GaAs occurred at $\lambda_s=2107$ nm and $\lambda_i=2150$ nm ($t_{\mathrm{PPLN}}=82.7$°C), corresponding to the frequency offset of 2.8 THz. This agreed with the calculated, as well as measured,[14] GaAs QPM peak position at a QPM period of 504 μm. Our estimate of the THz-wave bandwidth of ~300 GHz was based on optical-wave linewidth measurements: the THz spectrum was a convolution of two optical spectra, each ~200 GHz wide. With signal and idler polarizations of [001] and [110], respectively, the polarization of the THz beam was measured to be along the [110] crystalline direction of GaAs, in agreement with the symmetry of the EO tensor.[19]

The THz average power was measured with a calibrated DLaTGS pyroelectric detector (Bruker Optics) and black polyethylene filters, which blocked the optical radiation. The largest THz average output power of 1 mW was achieved when the DB-GaAs was placed 2 cm beyond the focused signal and idler beam waists (toward M8) at a position where the spot sizes were each $w_1=173$ μm. Figure 3(a) shows the THz-beam intensity profile after collimating mirror M9, reconstructed from scanning knife-edge measurements. Horizontal and vertical $1/e^2$ spot sizes of 7.8 and 13.3 mm, respectively, were close to the diffraction limit (assuming $w_{\mathrm{THz}}=w_1/\sqrt{2}=122$ μm inside GaAs). The THz beam, measured in the focus of a $f=50$ mm Picarin lens, was captured [Fig. 3(b)] by a

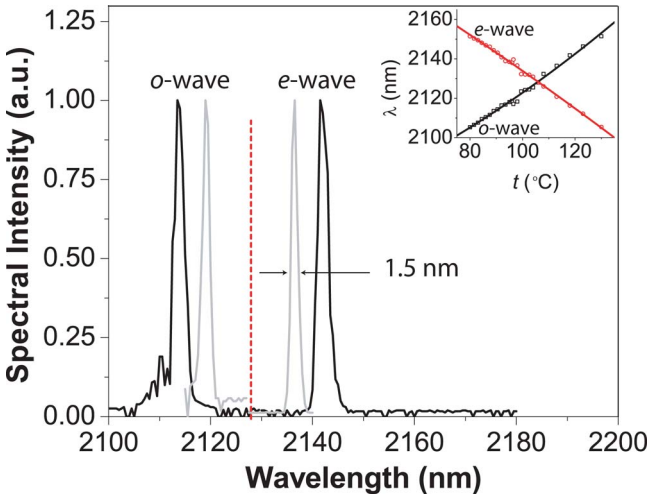

Fig. 2. (Color online) PPLN OPO line shapes near degeneracy for two different PPLN temperatures: $t=90$°C (frequency splitting of 2.05 THz, black lines) and $t=100$°C (frequency splitting of 0.96 THz, gray lines). The dotted line represents the degeneracy point (2128 nm). The inset shows OPO tuning curves as a function of the PPLN crystal temperature.

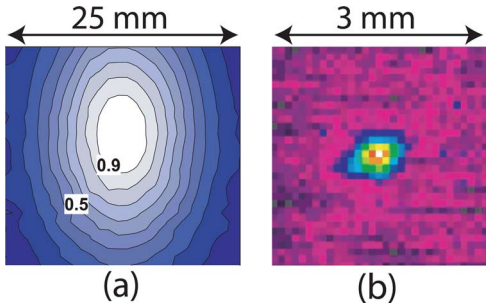

Fig. 3. (Color online) (a) Collimated THz-beam intensity profile reconstructed from scanning knife-edge measurements. (b) Focused (Picarin $f=50$ mm lens) THz-beam intensity profile measured by a room-temperature pyroelectric camera (1 pixel$=100\ \mu\text{m}\times 100\ \mu\text{m}$).

room-temperature pyroelectric camera (Pyrocam III, Spiricon). The focused beam spot is $\sim 2-3$ pixels (1 pixel$=100\ \mu\text{m}\times 100\ \mu\text{m}$), which again confirmed diffraction-limited performance.

Since the THz power scales as the product of the signal and idler powers, in the DRO case, it scales as the inverse square of the cavity loss. The OPO mirrors plus the PPLN crystal introduced round-trip intensity losses of 2.5%. The largest contributions to round-trip loss came from the DB-GaAs (12%) and the two polarizers (6–8%); therefore, the total round-trip intensity loss exceeded 20% for each resonating wave. The DRO threshold was 2.4 W. At the maximum pump power reaching the PPLN crystal of 8.5 W, the pump depletion was 67%, and the intracavity signal and idler average powers were 10.2 W and 17 W, respectively. Assuming that the signal and idler had the same pulse widths as the pump, we found that the generated 1 mW of THz output power was within ±10% of theoretical predictions.[20] Even with DRO round-trip losses greater than 20%, we achieved a 22-fold enhancement of the product of the signal and idler powers, as compared with extracavity THz generation (assuming with 67% conversion of 8.5 W of pump power, we would have generated $2.8\ \text{W}\times 2.8\ \text{W}$ of signal times idler outside the OPO cavity).

In conclusion, we demonstrated a room-temperature THz source using QPM GaAs with 1 mW average output power at 2.8 THz, based on intracavity difference-frequency mixing between the two resonating optical waves of a synchronously pumped DRO. With DRO round-trip intensity losses of 4.5%, 20 mW of THz radiation could be generated with a 8.5 W of pump power. We will employ a "dither-and-lock" technique to stabilize the DRO and generate a THz output with a duty factor of 100%.

This work was supported by DARPA under grant FA9550–04–01–0465. We thank L. Gordon for fabricating the DB-GaAs crystal. J. Schaar (jschaar@stanford.edu) acknowledges support from a Stanford Graduate Fellowship provided by Abbott Laboratories.

References

1. F. Zernike, Jr. and P. R. Berman, Phys. Rev. Lett. **15**, 999 (1965).
2. T. J. Bridges and A. R. Strnad, Appl. Phys. Lett. **20**, 382 (1972).
3. B. Lax, R. L. Aggarwal, and G. Favrot, Appl. Phys. Lett. **23**, 679 (1973).
4. W. Shi, Y. J. Ding, N. Fernelius, and K. Vodopyanov, Opt. Lett. **27**, 1454 (2002).
5. Y. Sasaki, Y. Avetisyan, K. Kawase, and H. Ito, Appl. Phys. Lett. **81**, 3323 (2002).
6. I. Tomita, H. Suzuki, H. Ito, H. Takenouchi, K. Ajito, R. Rungsawang, and Y. Ueno, Appl. Phys. Lett. **88**, 071118-1 (2006).
7. M. A. Piestrup, R. N. Fleming, and R. H. Pantell, Appl. Phys. Lett. **26**, 418 (1975).
8. K. Kawase, M. Sato, T. Taniuchi, and H. Ito, Appl. Phys. Lett. **68**, 2483 (1996).
9. T. J. Edwards, D. Walsh, M. B. Spurr, C. F. Rae, M. H. Dunn, and P. G. Browne, Opt. Express **14**, 1582 (2006).
10. L. Xu, X.-C. Zhang, and D. H. Auston, Appl. Phys. Lett. **61**, 1784 (1992).
11. Y.-S. Lee, T. Meade, V. Perlin, H. Winful, T. B. Norris, and A. Galvanauskas, Appl. Phys. Lett. **76**, 2505 (2000).
12. C. Weiss, G. Torosyan, Y. Avetisyan, and R. Beigang, Opt. Express **26**, 563 (2001).
13. A. Stepanov, J. Kuhl, I. Kozma, E. Riedle, G. Almási, and J. Hebling, Opt. Express **13**, 5762 (2005).
14. K. L. Vodopyanov, M. M. Fejer, X. Yu, J. S. Harris, Y.-S. Lee, W. C. Hurlbut, V. G. Kozlov, D. Bliss, and C. Lynch, Appl. Phys. Lett. **89**, 141119-1 (2006).
15. G. Imeshev, M. E. Fermann, K. L. Vodopyanov, M. M. Fejer, X. Yu, J. S. Harris, D. Bliss, and C. Lynch, Opt. Express **14**, 4439 (2006).
16. A. Mayer and F. Keilmann, Phys. Rev. B **33**, 6954 (1986).
17. L. A. Gordon, G. L. Woods, R. C. Eckardt, R. R. Route, R. S. Feigelson, M. M. Fejer, and R. L. Byer, Electron. Lett. **29**, 1942 (1993).
18. L. A. Eyres, P. J. Tourreau, T. J. Pinguet, C. B. Ebert, J. S. Harris, M. M. Fejer, L. Becouarn, B. Gerard, and E. Lallier, Appl. Phys. Lett. **79**, 904 (2001).
19. K. L. Vodopyanov, O. Levi, P. S. Kuo, T. J. Pinguet, J. S. Harris, M. M. Fejer, B. Gerard, L. Becouarn, and E. Lallier, Opt. Lett. **29**, 1912 (2004).
20. K. L. Vodopyanov, Opt. Express **14**, 2263 (2006).